

Heart Failure Therapy Mediated by the Trophic Activities of Bone Marrow Mesenchymal Stem Cells: A Non-invasive Therapeutic Regimen

Arsalan Shabbir, David Zisa, Gen Suzuki, and Techung Lee*

Department of Biochemistry and Center for Research in Cardiovascular Medicine

University at Buffalo, 3435 Main Street, Buffalo, NY 14214, USA

*Correspondence: Techung Lee, Department of Biochemistry, University at Buffalo,
3435 Main Street, Buffalo, NY 14214

(716) 829-3106; chunglee@buffalo.edu

Contract grant sponsor: NIH HL84590; NYSTEM

Running head: Non-invasive MSC therapeutics

Abstract

Heart failure carries a poor prognosis with few treatment options. While myocardial stem cell therapeutic trials have traditionally relied on intracoronary infusion or intramyocardial injection routes, these cell delivery methods are invasive and can introduce harmful scar tissue, arrhythmia, calcification, or microinfarction in the heart. Given that patients with heart failure are at an increased surgical risk, development of a non-invasive stem cell therapeutic approach is logistically appealing. Taking advantage of the trophic effects of bone marrow mesenchymal stem cells (MSCs) and using a hamster heart failure model, the present study demonstrates a novel non-invasive therapeutic regimen via direct delivery of MSCs into the skeletal muscle bed. Intramuscularly injected MSCs and MSC-conditioned medium each significantly improved ventricular function one month after MSC administration. MSCs at 4 million cells per animal increased fractional shortening by ~40%, enhanced capillary and myocyte nuclear density by ~30% and ~80%, attenuated apoptosis by ~60%, and reduced fibrosis by ~50%. Myocyte regeneration is evidenced by a ~2-fold increase in expression of cell cycle markers (Ki67 and phosphohistone H3) and ~13% reduction in mean myocyte diameter. Increased circulating levels of hepatocyte growth factor (HGF), leukemia inhibitory factor (LIF), and macrophage colony-stimulating factor (M-CSF) were associated with mobilization of c-kit⁺, CD31⁺, and CD133⁺ progenitor cells and subsequent increase in myocardial c-kit⁺ cells. Trophic effects of MSCs further activated expression of HGF, insulin-like growth factor-2 (IGF-2), and vascular endothelial growth factor (VEGF) in the myocardium. The work highlights a cardiac repair mechanism

mediated by trophic cross-talks between the injected MSCs, bone marrow, and heart that can be explored for non-invasive stem cell therapy.

Key words: heart failure, mesenchymal stem cells, trophic factors, non-invasive

Introduction

Advances in patient management and treatment have lowered death rates from heart disease over the last 30 years, but have led to an increasing patient population living with heart failure. Unfortunately, the only therapy available to reverse the decline in cardiac function is heart transplantation. However, this option is available to very few patients due to a shortage of donor hearts. Late sequela of immuno-suppression and rejection further limit the efficacy of this approach (4). Recent interests in stem cell therapeutics have prompted preclinical and clinical studies on the feasibility and safety of stem cells for treating heart disease (6, 46). Although mixed results have been documented without a clear consensus on the best cell for cardiac regeneration, the ease of large-scale cell expansion and immuno-privileged status of bone marrow mesenchymal stem cells (MSCs) are attractive features of the adult stem cells (13, 48, 57).

Myocardial stem cell therapy often uses invasive cell delivery approaches such as intramyocardial injection or intracoronary infusion. Given that patients with heart failure are at an increased surgical risk, development of a non-invasive cell delivery regimen is logistically appealing. A salient feature of MSCs is their ability to produce a plethora of trophic factors (7, 15), which may be harnessed for non-invasive stem cell therapy for heart failure. Indeed, documented cardiovascular beneficial effects of MSCs have largely been attributed to their paracrine actions independent of their differentiation potentials (14, 52, 56, 58). This recognition stems from the findings that efficiencies of myocardial recruitment and engraftment after local or systemic stem cell administration are typically too low to account for functional improvement. Our recent cell tracking study estimated

that only 1-2% of intracoronary-infused MSCs engrafted in the pig heart with no evidence of MSC differentiation into cardiomyocytes (32). Further, since diseased tissue environments often exhibit pathologic levels of ischemia, inflammation, and fibrosis, which can impair cell survival, therapeutic delivery of stem cells to areas away from the damaged heart offers a novel concept.

The multiple trophic factors produced by MSCs are capable of attenuating tissue injury, inhibiting fibrotic remodeling, promoting angiogenesis, stimulating recruitment and proliferation of tissue stem cells, or reducing inflammatory oxidative stress (7, 15, 34, 48). We hypothesize that MSCs, via secretion of these functionally synergistic trophic factors, are able to rescue the failing heart even when delivered away from the myocardium. Delivery of MSCs by intramuscular injection offers a feasible noninvasive strategy as skeletal muscle, being the most abundant tissue in the body, is amenable to repeated injection of large numbers of stem cells. Along this line, we have shown by PCR analysis that intramuscularly injected MSCs are trapped in the muscular bed with no detectable migration to other tissues (48). This cell injection regimen is used here to provide the ultimate proof that the trophic actions of MSCs underlie their cardiovascular therapeutic effects. Using a hamster heart failure model characterized by us and others (12, 16, 39, 45), we demonstrate for the first time that non-invasive administration of MSCs or MSC-derived trophic factors via intramuscular injection effectively rescues the failing heart through intricate tissue cross-talk mechanisms. This non-invasive stem cell administration regimen, if validated clinically, is expected to facilitate future stem cell therapy for heart failure.

Methods and Materials

Animals

F1B (normal) and TO2 (cardiomyopathic) male hamsters were obtained from Bio Breeders (Watertown, MA, USA). All procedures and protocols conformed to institutional guidelines for the care and use of animals in research.

Echocardiography

Echocardiographic measurements were performed in a blind-folded fashion, and were described in our recent work (39).

MSC culture and intramuscular implantation

Porcine bone marrow MSCs were isolated as described (34, 59). To produce MSC-conditioned serum-free medium, MSCs were plated on fibronectin-coated surface and grown to sub-confluency. Cells were then washed thoroughly with Hank's balanced salt solution (HBSS), and maintained in serum- and phenol red-free Minimal Essential Medium (MEM) for 24 hours. The conditioned medium was harvested, and filtered prior to use. For intramuscular implantation, MSCs (0.25, 1, or 4 million cells per animal) were resuspended in 0.8 ml HBSS, and injected in equally divided doses into the left and right hamstrings of 4-month old TO2 hamsters. Control TO2 hamsters received the same volume of HBSS. Animals received a second intramuscular MSC implantation two weeks later since preliminary cell injection trials indicated more prominent therapeutic effects with a repeated cell injection. For medium injection, TO2 hamsters received three weekly injections each of 0.8 ml of the conditioned medium for four weeks.

ELISA assay

Circulating cardiac Troponin-I (cTnI) was assayed with a rat cTnI ELISA kit (Life Diagnostics) using plasma samples collected one month after MSC administration. Assays of circulating leukemia inhibitory factor (LIF) and macrophage-colony stimulating factor (M-CSF) were performed using the MAP program (Rules-Based Medicine). Hepatocyte growth factor (HGF), vascular endothelial growth factor (VEGF), and insulin-like growth factor-2 (IGF-2) were analyzed by ELISA kits from R&D: mouse HGF DuoSet (#DY2207), rat VEGF DuoSet (#DY564), and mouse IGF-2 DuoSet (#DY792). Heart tissues were homogenized in an ice-cold lysis solution containing 0.1% TX-100 and 2 mM EDTA. Lysates were clarified, diluted to 1 mg proteins/ml, and used for ELISA per manufacturer's instructions.

Flow cytometry

Peripheral blood mononuclear cells were isolated three days after MSC administration, and red blood cells were removed by a lysis buffer (150 mM NH₄Cl, 10 mM KHCO₃, and 0.1 mM EDTA). Cells were washed and resuspended in normal saline. After blocking with an FcR receptor blocker for 30 minutes, cells were labeled with PE-conjugated CD133 (#AC133; Miltenyi Biotec), PE-conjugated CD31 (#12-0311; eBioscience), and PE-conjugated c-kit (#12-1171; eBioscience) antibodies. Flow cytometry was performed on ~25,000 cells and data were analyzed using FCS Express (De Novo Software). Proper isotype-matched immunoglobulins were used as controls. Dead cells were excluded by 7-amino-actinomycin D (7-AAD) counterstaining.

Quantification of capillary and cardiomyocyte nuclear density

Freshly excised tissues were immersed in OCT, frozen in liquid nitrogen, and stored at -80°C until use. Ventricular cross sections $5\ \mu\text{m}$ thick were obtained using a cryostat, fixed in acetone:ethanol mixture (3:1 ratio) for 5 minutes. Sections were blocked with Serum Free Protein Block (Dako) for 30 minutes. FITC-labeled GSL-IB4 lectin diluted 1:100 was incubated with the tissue sections overnight at 4°C . Cardiomyocytes were stained with a rabbit TnI antibody (#sc15368; Santa Cruz) the next day for 3 hours. The TnI antibody reacts with both cardiac and skeletal TnI of rodent and human origin. Sections were then incubated with a Texas Red conjugated anti-rabbit secondary antibody for 1 hour and then mounted using Vectashield's Mounting Medium with DAPI (Vector Laboratories). Images were taken in 15-25 random fields using Zeiss's Axioimager fluorescence microscope at 200x magnification. The number of capillaries (FITC channel) and total nuclei count (DAPI channel) were quantified by ImageJ software using the analyze particle feature. Non-cardiomyocyte nuclei quantified from the merged images by their lack of TnI staining were subtracted from total nuclei count to determine cardiomyocyte nuclear density. Black areas from images were subtracted using Photoshop aided quantification of black pixels to calculate total tissue area. Capillary and cardiomyocyte nuclear density were normalized to total tissue area in mm^2 .

Quantification of apoptosis

Analysis of apoptosis was performed on frozen sections prepared as described above using the ApopTag kit (Millipore) per manufacturer's instructions. TnI antibody was used to identify apoptotic myocytes and analysis was performed similarly as described above. All apoptotic nuclei in each section were counted and normalized to total myocytes and non-myocytes.

Quantification of fibrosis and cardiomyocyte diameter

Masson-Trichrome sections were used for fibrosis analysis and cardiomyocyte diameters. Fibrosis was performed by Photoshop-aided quantification of image pixels. The blue color range was selected to represent fibrotic areas. At least 15 random fields at 200x magnification were assessed for each slide by three independent examiners with one being blind-folded. Artifactual spaces (white clear areas) from images were subtracted using Photoshop aided quantification of white pixels to calculate total tissue area. The ratio of fibrotic areas to total tissue areas was calculated as % fibrotic areas. For quantification of cardiomyocyte diameters, at least 350 random cardiomyocytes were measured for each animal using AxioVision LE software's measurement tool (Carl Zeiss, Germany).

Quantification of c-kit⁺, Ki67⁺ and phosphohistone H3⁺ cells

Paraformaldehyde-fixed, paraffin-embedded heart sections 5 μm thick were utilized for c-kit, Ki-67, and phosphohistone H3 (p-HH3) staining. Antigen retrieval was done by steaming in 10 mM citrate (pH 6) for 30 minutes followed by permeabilization in 1% TritonX-100 for 20 minutes. Sections were blocked with a normal saline

supplemented with 0.025% TW-20 and 2% non-fat milk powder for 30 minutes and incubated with diluted primary antibody overnight. Primary antibodies used were: c-kit antibody (#A4502; DAKO), Ki67 antibody (#RM-9106; Thermo Scientific), and p-HH3 antibody (#07-145; Millipore). Myocytes were stained with a mouse cardiac TnT antibody (#MS-295; Thermo Scientific) the next day for 1 hour. The cTnT antibody reacts with cTnT of multiple species. The Sections were then incubated with an Alexa-647 conjugated anti-rabbit and Alexa-488 conjugated anti-mouse secondary antibodies for 30 minutes and then mounted in Vectashield's Mounting Medium with DAPI. Sections were analyzed as described above using Zeiss's Axioimager fluorescence microscope at 200x magnification.

Real time qRT-PCR

RNA isolation and qRT-PCR protocols were as described (34). β 2-microglobulin (B2M) was used as the reference gene for calculations. Injected MSCs were quantified by pig-specific 16S rRNA primers. A standard curve was created by generating a serial dilution curve plotting the threshold cycles of the 16s rRNA gene against known number of MSCs. The primer sequences are listed in Table 1.

Statistical analysis

Data were expressed as means \pm SEM. Comparisons were based on unpaired Student's t test. A value of $P < 0.05$ was considered significant.

Results

Hamster heart failure model. The TO2 hamster strain harbors a genetic defect in the δ -sarcoglycan gene, which causes dilated cardiomyopathy leading to congestive heart failure clinically identical to that occurring in the general category of human heart failure (12, 16, 45). Functional deterioration of the TO2 heart is accompanied by prominent myocyte loss, inflammation, fibrosis, and calcified lesions (44, 45). We show that left ventricular ejection fraction (LVEF) and fractional shortening (FS) of the TO2 hamster heart decline by approximately 25% and 35%, respectively, at 4 months of age (39). MSC therapeutic trials described here were performed using 4-month old TO2 hamsters.

Non-invasive MSC delivery for heart failure. Preclinical and clinical studies of myocardial stem cell therapy often use invasive cell delivery approaches such as intramyocardial injection or intracoronary infusion. Given that patients with heart failure are at an increased surgical risk, it is logistically appealing to explore a non-invasive cell delivery approach. MSCs, via their ability of trophic factor production, may be harnessed toward achieving the goal. Using both histological and PCR detection methods, we have recently shown that intramuscularly injected MSCs are largely trapped in the musculature with no detectable cell migration to other tissues including the heart (48). This non-invasive cell injection regimen takes advantage of the fact that skeletal muscle is the largest tissue of the body and is amenable to repeated injections, which is difficult to achieve with myocardial cell delivery routes. To address the feasibility of intramuscular injection of MSCs for heart failure, we first carried out cell dosage studies comparing

injections of 0.25, 1, and 4 million MSCs into the hamstring muscle of TO2 cardiomyopathic hamsters. Blind-folded echocardiography was performed one month after cell injection, showing that all three MSC dosage groups significantly improved ventricular function and attenuated chamber dilation (Fig. 1A-B). The 4-million dosage group clearly exhibited the most prominent functional improvement as indicated by a ~40% increase in fractional shortening (FS) and ~10% decrease in left ventricular diastolic diameter (LVDd). The 4-million dosage group also caused a ~80% increase in systolic wall thickening (data not shown).

Since MSC migration to the heart was undetectable after the intramuscular injection (48), the observed functional improvement must have been mediated by trophic factors. To provide the evidence, MSC-conditioned medium was used to determine whether administration of cell-free medium would similarly rescue the failing heart. The medium was administered by multiple injections into the hamstring muscle, and echocardiography was performed after one month. The study showed that MSC-conditioned medium was again effective in improving ventricular function and decreasing dilation when compared to the control medium (Fig. 1C-D). These functional studies thus demonstrated the feasibility of non-invasive MSC therapy for heart failure using the convenient intramuscular injection route.

Active regeneration of the failing heart. Histological studies were further performed to ascertain that functional improvement caused by intramuscularly injected MSCs is associated with myocardial tissue regeneration. We found that capillary and

myocyte nuclear density in the MSC treatment group was ~30% and ~80% higher than the control injection group, respectively (Fig. 2A-C). Higher myocyte nuclear density can be contributed by newly regenerated myocytes, which are typically smaller (37, 48). Figure 2D indeed shows that the mean cross-section myocyte diameter was smaller in the MSC-treated group ($15.8 \pm 0.9 \mu\text{m}$) than the control group ($18.2 \pm 0.3 \mu\text{m}$). The frequency histogram depicts a shift toward smaller myocyte diameters in the MSC group, suggesting prominent presence of newly regenerated myocytes (Fig. 2E). To provide additional evidence along this line, we quantified two specific markers associated with cell cycle activity: Ki67 and phosphohistone H3 (p-HH3) (18, 33). Quantitative analyses showed that expression of Ki67 (Fig. 3A-C) and p-HH3 (Fig. 3D-F) were increased by ~2 fold in the MSC group, and that increased expression of the cell cycle markers could be detected in both myocyte and non-myocyte populations. Thus, cardiac functional improvement after intramuscular injection of MSCs is mediated by active myocardial regeneration.

Down-regulation of apoptosis and tissue injury. Since many trophic factors produced by MSCs possess anti-apoptotic function (7, 15), the observed myocardial tissue regeneration could also be contributed by reduced apoptosis. Histological analysis of myocardial tissue sections revealed that MSCs decreased apoptosis of myocytes and non-myocytes each by ~60% (Fig. 4A-B), suggesting that trophic factors promoted cell survival in the myocardium. Consistent with this finding, circulating cardiac TnI levels were decreased by ~60% (MSC group vs. saline control group: $1.8 \pm 0.25 \text{ ng/ml}$ vs. $4.49 \pm 0.9 \text{ ng/ml}$) (Fig. 4C), reflecting significant attenuation of myocardial tissue injury.

Attenuation of pathologic fibrosis. The TO2 cardiomyopathic hamster heart exhibits progressive fibrosis marked by elevated expression of collagens, metalloproteinases (MMPs), and tissue inhibitor of MMPs (TIMPs) (11, 44, 45). Examinations of histological sections revealed greatly diminished left ventricular fibrosis and leukocyte infiltration after MSC treatment (Fig. 5A). Fibrotic areas in the TO2 saline control group were ~12%, in contrast to ~1% fibrotic areas in the normal F1B hamster heart. MSC injection caused a ~50% decrease in fibrosis in the TO2 heart (Fig. 5B). Since the balance between collagen synthesis and degradation is mediated by MMPs and TIMPs, and is of crucial relevance in maintaining myocardial structural integrity (49), we further used qRT-PCR to assess the expression of these molecular players. Figure 5C shows that the control TO2 heart exhibited elevated expression of collagens, MMP's, and TIMP's as shown previously (11), and MSC administration reversed the abnormal expression profiles of collagens, MMP's, and TIMP's. Thus, the non-invasive delivery of MSCs, through trophic activities, rescued the failing heart by improving ventricular function, promoting myocardial tissue regeneration and survival, and attenuating pathologic fibrosis.

Increased circulating and myocardial trophic factors. We next sought to identify the therapeutic mechanisms mediated by the intramuscularly injected MSCs. The multiple trophic factors produced by MSCs are known to possess functionally synergistic and redundant activities that are beneficial to the heart (7, 15, 34). The trophic factors may be initially released from the intramuscularly injected MSCs and subsequently affect the expression of growth factors in the myocardium. Several major

growth factors and cytokines present in the plasma and heart tissue homogenates were analyzed by ELISA one month after MSC administration. These immunoassays revealed increased circulating levels of hepatocyte growth factor (HGF), leukemia inhibitory factor (LIF), and macrophage-colony stimulating factor (M-CSF) in the MSC treatment group (Fig. 6A). Elevated expression of HGF, insulin-like growth factor-2 (IGF-2), and vascular endothelial growth factor (VEGF) in the myocardium were further identified by both ELISA (Fig. 6B) and qRT-PCR (data not shown), indicating that trophic activities of MSCs could amplify the expression of host growth factor genes in the myocardium.

Mobilization of bone marrow progenitor cells. Mobilization of bone marrow progenitor cells plays an important role in tissue repair (30). Among the multiple MSC trophic factors, HGF, VEGF, G/M-CSF, stem cell factor (SCF), IGF, and stromal-derived factor-1 (SDF-1) are known to be able to mobilize bone marrow progenitor cells (19, 23, 24, 28, 29, 31). Along this line, we have demonstrated that the MSCs used in the current study express IGF-2, LIF, G/M-CSF, SDF-1, and VEGF (34, 59). We therefore investigated whether bone marrow progenitor cells might be mobilized in response to the injected MSCs. Flow cytometric analysis of peripheral blood indeed showed that MSCs significantly increased circulating progenitor cells expressing c-kit, CD31, or CD133 surface markers (Fig. 7), which have been shown to originate from the bone marrow compartment and contribute to tissue repair (21). A contribution by the injected MSCs to these circulating progenitor cells can be ruled out because we and others have shown that intramuscularly injected MSCs are trapped in the musculature with no detectable

migration (10, 48) and that MSCs do not express the c-kit (CD117), CD31, and CD133 markers (1, 59).

Myocardial c-kit⁺ progenitor cells. Mobilized bone marrow progenitor cells are thought to participate in tissue repair through tissue homing mechanisms (19, 21, 30). Increased capillary and myocyte densities as shown in Figure 2 could be mediated by myocardial recruitment and subsequent differentiation of circulating progenitor cells, some of which have been found to express the c-kit marker (3). To explore this possibility, we further examined whether the myocardium might harbor elevated pools of c-kit⁺ progenitor cells after MSC administration. Immunostaining revealed a ~2-fold increase after MSC administration in ventricular c-kit⁺ cells (Fig. 8A-B). This increase was further corroborated by qRT-PCR analysis of myocardial c-kit expression (Fig. 8C). Thus, MSC-mediated mobilization of bone marrow progenitor cells is coupled with increased myocardial c-kit⁺ progenitor cells. Taken together, the non-invasive cell therapeutic regimen for heart failure takes advantage of the powerful trophic activities of MSCs, resulting in functional improvement and myocardial regeneration.

Discussion

The present study demonstrates a novel non-invasive MSC therapeutic regimen for heart failure based on intramuscular delivery route. The intramuscularly injected MSCs or MSC-conditioned medium improved ventricular function, promoted myocardial regeneration, attenuated apoptosis and fibrotic remodeling, recruited bone marrow progenitor cells, and induced myocardial expression of multiple growth factor genes. These findings highlight the critical cross-talks between the injected MSCs and host tissues, culminating in effective cardiac repair for the failing hamster heart.

Advantages of intramuscular MSC delivery

Patients with heart failure are at an increased surgical risk. While most stem cell trials have used intracoronary infusion or intramyocardial injection for cell delivery, these delivery methods are invasive, often clinically unsuitable, and can introduce harmful scar tissue, arrhythmia, calcification, or microinfarction in the heart (5, 60-62). Systemic delivery by intravenous infusion of MSCs has been found to cause entrapment of MSCs in the lungs (2). An important issue to consider is whether the engrafted stem cells may become electromechanically coupled with resident cardiomyocytes. Myoblasts for instance do not exhibit optimal electrophysiological integration upon myocardial engraftment, leading to post-implantation arrhythmogenesis (38). Successful clinical applications may be more feasible with a non-invasive approach, delivering MSCs to areas away from the damaged heart. Given the powerful trophic effects of MSCs, delivery of MSCs via an intramuscular route may be a superior noninvasive strategy, allowing repeated administration of large numbers of cells and circumventing

entrapments and dilution by other tissue. In addition, since we and others have shown that MSC treatment ameliorates muscular dystrophy (9, 35, 48), intramuscular injection of MSCs is expected to be well suited for treating muscular dystrophy patients with cardiomyopathies.

Cardiac repair mediated by trophic mechanisms

While early preclinical studies suggested therapeutic mechanisms mediated by stem cell trans-differentiation or fusion (42, 55), it has become apparent that these mechanisms do not occur in sufficiently high frequency to account for the observed functional improvement after stem cell administration (15). Our cell tracking study estimated that only 1-2% of intracoronary-infused MSCs engrafted in the pig heart (32), and yet this low efficiency of cell engraftment was able to significantly improve function in the porcine hibernating myocardium (50). We note that although systemic delivery of MSCs by intravenous infusion caused cell entrapment in the lungs (2), this cell delivery strategy was found to improve cardiac function in rats with acute myocardial infarction (40). These findings are consistent with increasing evidence suggesting that the cardiovascular beneficial effects of stem cell therapy are largely due to the actions of trophic factors or paracrine mediators (14, 53, 56). In addition, studies have attributed trophic activities of myoblasts and endothelial progenitor cells as critical cardioprotective mechanisms (20, 43). Our demonstration here that the intramuscularly injected MSCs and MSC-conditioned medium are both therapeutically effective for treating hamster heart failure provides the ultimate proof for the critical role of trophic factors in stem cell therapy. While various single growth factor therapeutic regimens have been attempted

for FGF, HGF, IGF, and VEGF with encouraging results (36, 41, 47, 51), the MSC therapy is unique in its engagement of functionally synergistic and redundant trophic factors (7, 15), which may be required for activation of the endogenous stem cell repair mechanism and a more sustained therapeutic effect.

Molecular cross-talks between MSCs and host tissues

Mobilization of bone marrow progenitor cells plays an important role in tissue repair (30). The MSCs used here have been shown to express trophic factors such as HGF, LIF, G/M-CSF, SDF-1, and VEGF (34, 59), which are capable of mobilizing bone marrow progenitor cells. Along this line, administration of G-CSF has been proposed as a potential new therapy for myocardial infarction (22), and intramuscular injection of LIF plasmid DNA has been found to be cardioprotective (63). We indeed detected elevated levels of circulating HGF, LIF, and M-CSF in the MSC-treated animals, and consistent with this finding, circulating c-kit⁺, CD31⁺, and CD133⁺ bone marrow progenitor cells were increased after MSC administration. Although unrestrained MSC secretions may cause an abnormally abundant mobilization of progenitor cells, this effect of MSCs is unlikely to be sustained because we observed a progressive loss of the injected MSCs (48). The mobilized progenitor cells can repopulate the myocardium, as shown here by increased myocardial c-kit⁺ progenitor cells, and participate in endogenous cardiac repair mechanisms. Notably, we have obtained evidence that this cell mobilization mechanism becomes impaired in the aged TO2 hamsters, which may explain at least in part why the MSC therapeutic regimen fails to rescue the aging heart (data not shown). This molecular cross-talk between the injected MSCs and bone marrow compartment thus

illustrates the dynamic and functionally relevant signaling cascade involved in stem cell repair. The signaling cascade depicted here can further activate myocardial expression of HGF, IGF, and VEGF genes, highlighting an additional cross-talk circuit between MSCs and the myocardium. Similar to this finding, Cho et al demonstrated that myocardial expression of several growth factor genes, including HGF, IGF, and VEGF, was up-regulated after intramyocardial stem cell implantation (8). Tateno et al found that implanted stem cells stimulated muscle cells to produce angiogenic factors that resulted in neovascularization (54). Our finding here is consistent with previous reports demonstrating that HGF administration could improve cardiac function in the TO2 cardiomyopathic hamsters (27, 41). Work is in progress to characterize the role and response of host tissues following MSC administration.

Exploring the immunomodulatory property of MSCs

MSCs are thought to possess unique immunomodulatory properties that can be explored for non-autologous or xenogeneic stem cell-based therapeutics (17, 57). The trophic action of MSCs can decrease host production of inflammatory cytokines and induce T cell anergy. The immune phenotype of culture-expanded MSCs is widely described as MHC Class I⁺, MHC Class II⁻, CD40⁻, CD80⁻, and CD86⁻, which is regarded as non-immunogenic, suggesting that MSCs are capable of trespassing species defense barriers. The use of MSCs in allogeneic and xenogeneic transplantation can reduce the incidence and severity of graft-vs-host disease (57). In this aspect, we have recently demonstrated that intramuscularly injected human and porcine MSCs are well tolerated by the TO2 dystrophic hamsters, and the MSC treatment leads to prominent skeletal

muscle regeneration and attenuates oxidative stress without inflaming the host immune system (48). Given that stem cell function and potency can be impaired by aging and disease (25, 26), the use of non-autologous human MSCs isolated from healthy donors offers a major advantage since these adult stem cells can be routinely expanded in culture and thoroughly tested in advance for clinical applications.

Acknowledgments

The work is supported by NIH (R01HL84590) and New York State Stem Cell (NYSTEM) Program. We thank Dr. J. Canty for helpful discussion, and Merced Leiker and Huey Lin for technical assistance.

References

1. Baddoo M, Hill K, Wilkinson R, Gaupp D, Hughes C, Kopen GC, and Phinney DG. Characterization of mesenchymal stem cells isolated from murine bone marrow by negative selection. *J Cell Biochem* 89: 1235-1249, 2003.
2. Barbash IM, Chouraqui P, Baron J, Feinberg MS, Etzion S, Tessone A, Miller L, Guetta E, Zipori D, Kedes LH, Kloner RA, and Leor J. Systemic delivery of bone marrow-derived mesenchymal stem cells to the infarcted myocardium: feasibility, cell migration, and body distribution. *Circulation* 108: 863-868, 2003.
3. Bearzi C, Rota M, Hosoda T, Tillmanns J, Nascimbene A, De Angelis A, Yasuzawa-Amano S, Trofimova I, Siggins RW, Lecapitaine N, Cascapera S, Beltrami AP, D'Alessandro DA, Zias E, Quaini F, Urbanek K, Michler RE, Bolli R, Kajstura J, Leri A, and Anversa P. Human cardiac stem cells. *Proc Natl Acad Sci U S A* 104: 14068-14073, 2007.
4. Brann WM, Bennett LE, Keck BM, and Hosenpud JD. Morbidity, functional status, and immunosuppressive therapy after heart transplantation: an analysis of the joint International Society for Heart and Lung Transplantation/United Network for Organ Sharing Thoracic Registry. *J Heart Lung Transplant* 17: 374-382, 1998.
5. Breitbach M, Bostani T, Roell W, Xia Y, Dewald O, Nygren JM, Fries JW, Tiemann K, Bohlen H, Hescheler J, Welz A, Bloch W, Jacobsen SE, and Fleischmann BK. Potential risks of bone marrow cell transplantation into infarcted hearts. *Blood* 110: 1362-1369, 2007.
6. Burt RK, Loh Y, Pearce W, Beohar N, Barr WG, Craig R, Wen Y, Rapp JA, and Kessler J. Clinical applications of blood-derived and marrow-derived stem cells for nonmalignant diseases. *Jama* 299: 925-936, 2008.
7. Caplan AI, and Dennis JE. Mesenchymal stem cells as trophic mediators. *J Cell Biochem* 98: 1076-1084, 2006.
8. Cho HJ, Lee N, Lee JY, Choi YJ, Ii M, Wecker A, Jeong JO, Curry C, Qin G, and Yoon YS. Role of host tissues for sustained humoral effects after endothelial progenitor cell transplantation into the ischemic heart. *J Exp Med* 204: 3257-3269, 2007.
9. De Bari C, Dell'Accio F, Vandenabeele F, Vermeesch JR, Raymackers JM, and Luyten FP. Skeletal muscle repair by adult human mesenchymal stem cells from synovial membrane. *J Cell Biol* 160: 909-918, 2003.
10. Dezawa M, Ishikawa H, Itokazu Y, Yoshihara T, Hoshino M, Takeda S, Ide C, and Nabeshima Y. Bone marrow stromal cells generate muscle cells and repair muscle degeneration. *Science* 309: 314-317, 2005.
11. Dixon IM, Ju H, Reid NL, Scammell-La Fleur T, Werner JP, and Jasmin G. Cardiac collagen remodeling in the cardiomyopathic Syrian hamster and the effect of losartan. *J Mol Cell Cardiol* 29: 1837-1850, 1997.
12. Fiaccavento R, Carotenuto F, Minieri M, Fantini C, Forte G, Carbone A, Carosella L, Bei R, Masuelli L, Palumbo C, Modesti A, Prat M, and Di Nardo P. Stem cell activation sustains hereditary hypertrophy in hamster cardiomyopathy. *J Pathol* 205: 397-407, 2005.

13. Giordano A, Galderisi U, and Marino IR. From the laboratory bench to the patient's bedside: an update on clinical trials with mesenchymal stem cells. *J Cell Physiol* 211: 27-35, 2007.
14. Gneocchi M, He H, Noiseux N, Liang OD, Zhang L, Morello F, Mu H, Melo LG, Pratt RE, Ingwall JS, and Dzau VJ. Evidence supporting paracrine hypothesis for Akt-modified mesenchymal stem cell-mediated cardiac protection and functional improvement. *Faseb J* 20: 661-669, 2006.
15. Gneocchi M, Zhang Z, Ni A, and Dzau VJ. Paracrine mechanisms in adult stem cell signaling and therapy. *Circ Res* 103: 1204-1219, 2008.
16. Goineau S, Pape D, Guillo P, Ramee M-P, and Bellissant E. Hemodynamic and histomorphometric characteristics of dilated cardiomyopathy of Syrian hamsters (Bio TO-2 strain). *Can J Physiol Pharmacol* 79: 329-337, 2001.
17. Gotherstrom C. Immunomodulation by multipotent mesenchymal stromal cells. *Transplantation* 84: S35-37, 2007.
18. Goto H, Tomono Y, Ajiro K, Kosako H, Fujita M, Sakurai M, Okawa K, Iwamatsu A, Okigaki T, Takahashi T, and Inagaki M. Identification of a novel phosphorylation site on histone H3 coupled with mitotic chromosome condensation. *J Biol Chem* 274: 25543-25549, 1999.
19. Haider H, Jiang S, Idris NM, and Ashraf M. IGF-1-overexpressing mesenchymal stem cells accelerate bone marrow stem cell mobilization via paracrine activation of SDF-1alpha/CXCR4 signaling to promote myocardial repair. *Circ Res* 103: 1300-1308, 2008.
20. Hinkel R, El-Aouni C, Olson T, Horstkotte J, Mayer S, Muller S, Willhauck M, Spitzweg C, Gildehaus FJ, Munzing W, Hannappel E, Bock-Marquette I, DiMaio JM, Hatzopoulos AK, Boekstegers P, and Kupatt C. Thymosin beta4 is an essential paracrine factor of embryonic endothelial progenitor cell-mediated cardioprotection. *Circulation* 117: 2232-2240, 2008.
21. Hristov M, Erl W, and Weber PC. Endothelial progenitor cells: isolation and characterization. *Trends Cardiovasc Med* 13: 201-206, 2003.
22. Ince H, Petzsch M, Kleine HD, Schmidt H, Rehders T, Korber T, Schumichen C, Freund M, and Nienaber CA. Preservation from left ventricular remodeling by front-integrated revascularization and stem cell liberation in evolving acute myocardial infarction by use of granulocyte-colony-stimulating factor (FIRSTLINE-AMI). *Circulation* 112: 3097-3106, 2005.
23. Ishizawa K, Kubo H, Yamada M, Kobayashi S, Suzuki T, Mizuno S, Nakamura T, and Sasaki H. Hepatocyte growth factor induces angiogenesis in injured lungs through mobilizing endothelial progenitor cells. *Biochem Biophys Res Commun* 324: 276-280, 2004.
24. Kalka C, Masuda H, Takahashi T, Gordon R, Tepper O, Gravereaux E, Pieczek A, Iwaguro H, Hayashi SI, Isner JM, and Asahara T. Vascular endothelial growth factor(165) gene transfer augments circulating endothelial progenitor cells in human subjects. *Circ Res* 86: 1198-1202, 2000.
25. Keymel S, Kalka C, Rassaf T, Yeghiazarians Y, Kelm M, and Heiss C. Impaired endothelial progenitor cell function predicts age-dependent carotid intimal thickening. *Basic Res Cardiol* 103: 582-586, 2008.

26. Kissel CK, Lehmann R, Assmus B, Aicher A, Honold J, Fischer-Rasokat U, Heeschen C, Spyridopoulos I, Dimmeler S, and Zeiher AM. Selective functional exhaustion of hematopoietic progenitor cells in the bone marrow of patients with postinfarction heart failure. *J Am Coll Cardiol* 49: 2341-2349, 2007.
27. Kondoh H, Sawa Y, Fukushima N, Matsumiya G, Miyagawa S, Kitagawa-Sakakida S, Imanishi Y, Kawaguchi N, Matsuura N, and Matsuda H. Combined strategy using myoblasts and hepatocyte growth factor in dilated cardiomyopathic hamsters. *Ann Thorac Surg* 84: 134-141, 2007.
28. Korbling M. In vivo expansion of the circulating stem cell pool. *Stem Cells* 16 Suppl 1: 131-138, 1998.
29. Kucia M, Zhang YP, Reza R, Wysoczynski M, Machalinski B, Majka M, Ildstad ST, Ratajczak J, Shields CB, and Ratajczak MZ. Cells enriched in markers of neural tissue-committed stem cells reside in the bone marrow and are mobilized into the peripheral blood following stroke. *Leukemia* 20: 18-28, 2006.
30. LaBarge MA, and Blau HM. Biological progression from adult bone marrow to mononucleate muscle stem cell to multinucleate muscle fiber in response to injury. *Cell* 111: 589-601, 2002.
31. Lehrke S, Mazhari R, Durand DJ, Zheng M, Bedja D, Zimmet JM, Schuleri KH, Chi AS, Gabrielson KL, and Hare JM. Aging impairs the beneficial effect of granulocyte colony-stimulating factor and stem cell factor on post-myocardial infarction remodeling. *Circ Res* 99: 553-560, 2006.
32. Leiker M, Suzuki G, Iyer VS, Canty JM, and Lee T. Assessment of a Nuclear Affinity Labeling Method for Tracking Implanted Mesenchymal Stem Cells. *Cell Transplantation* 17: 911-922, 2008.
33. Leonardi E, Girlando S, Serio G, Mauri FA, Perrone G, Scampini S, Dalla Palma P, and Barbareschi M. PCNA and Ki67 expression in breast carcinoma: correlations with clinical and biological variables. *J Clin Pathol* 45: 416-419, 1992.
34. Lin H, Shabbir A, Molnar M, Yang J, Marion S, Canty JM, and Lee T. Adenoviral expression of vascular endothelial growth factor splice variants differentially regulate bone marrow-derived mesenchymal stem cells. *J Cell Physiol* 216: 458-468, 2008.
35. Liu Y, Yan X, Sun Z, B C, Q H, J L, and C ZR. Flk-1+ adipose-derived mesenchymal stem cells differentiate into skeletal muscle satellite cells and ameliorate muscular dystrophy in mdx mice. *Stem Cells Dev* 16: 695-706, 2007.
36. Losordo DW, Vale PR, Symes JF, Dunnington CH, Esakof DD, Maysky M, Ashare AB, Lathi K, and Isner JM. Gene therapy for myocardial angiogenesis: initial clinical results with direct myocardial injection of phVEGF165 as sole therapy for myocardial ischemia. *Circulation* 98: 2800-2804, 1998.
37. Lynch P, Lee TC, Fallavollita JA, Canty JM, Jr., and Suzuki G. Intracoronary administration of AdvFGF-5 (fibroblast growth factor-5) ameliorates left ventricular dysfunction and prevents myocyte loss in swine with developing collaterals and ischemic cardiomyopathy. *Circulation* 116: 171-76, 2007.
38. Menasche P, Hagege AA, Vilquin JT, Desnos M, Abergel E, Pouzet B, Bel A, Sarateanu S, Scorsin M, Schwartz K, Bruneval P, Benbunan M, Marolleau

- JP, and Duboc D. Autologous skeletal myoblast transplantation for severe postinfarction left ventricular dysfunction. *J Am Coll Cardiol* 41: 1078-1083, 2003.
39. Missihoun C, Zisa D, Shabbir A, Lin H, and Lee T. Myocardial oxidative stress, osteogenic phenotype, and energy metabolism are differentially involved in the initiation and early progression of delta-sarcoglycan-null cardiomyopathy. *Mol Cell Biochem* 321: 45-52, 2008.
40. Nagaya N, Fujii T, Iwase T, Ohgushi H, Itoh T, Uematsu M, Yamagishi M, Mori H, Kangawa K, and Kitamura S. Intravenous administration of mesenchymal stem cells improves cardiac function in rats with acute myocardial infarction through angiogenesis and myogenesis. *Am J Physiol Heart Circ Physiol* 287: H2670-2676, 2004.
41. Nakamura T, Matsumoto K, Mizuno S, Sawa Y, Matsuda H, and Nakamura T. Hepatocyte growth factor prevents tissue fibrosis, remodeling, and dysfunction in cardiomyopathic hamster hearts. *Am J Physiol Heart Circ Physiol* 288: H2131-2139, 2005.
42. Orlic D, Kajstura J, Chimenti S, Jakoniuk I, Anderson SM, Li B, Pickel J, McKay R, Nadal-Ginard B, Bodine DM, Leri A, and Anversa P. Bone marrow cells regenerate infarcted myocardium. *Nature* 410: 701-705, 2001.
43. Perez-Illarbe M, Agbulut O, Pelacho B, Ciorba C, San Jose-Eneriz E, Desnos M, Hagege AA, Aranda P, Andreu EJ, Menasche P, and Prosper F. Characterization of the paracrine effects of human skeletal myoblasts transplanted in infarcted myocardium. *Eur J Heart Fail* in press: 2008.
44. Ryoke T, Gu Y, Ikeda Y, Martone ME, Oh SS, Jeon ES, Knowlton KU, and Ross J, Jr. Apoptosis and oncosis in the early progression of left ventricular dysfunction in the cardiomyopathic hamster. *Basic Res Cardiol* 97: 65-75, 2002.
45. Sakamoto A, Ono K, Abe M, Jasmin G, Eki T, Murakami Y, Masaki T, Toyo-Oka T, and Hanaoka F. Both hypertrophic and dilated cardiomyopathies are caused by mutation of the same gene, delta-sarcoglycan, in hamster: an animal model of disrupted dystrophin-associated glycoprotein complex. *Proc Natl Acad Sci U S A* 94: 13873-13878, 1997.
46. Segers VF, and Lee RT. Stem-cell therapy for cardiac disease. *Nature* 451: 937-942, 2008.
47. Serosé A, Prudhon B, Salmon A, Doyennette MA, Fiszman MY, and Fromes Y. Administration of insulin-like growth factor-1 (IGF-1) improves both structure and function of delta-sarcoglycan deficient cardiac muscle in the hamster. *Basic Res Cardiol* 100: 161-170, 2005.
48. Shabbir A, Zisa D, Leiker M, Johnston C, Lin H, and Lee T. Muscular dystrophy therapy by non-autologous mesenchymal stem cells: muscle regeneration without immunosuppression and inflammation. *Transplantation* in press: 2009.
49. Spinale FG, Coker ML, Heung LJ, Bond BR, Gunasinghe HR, Etoh T, Goldberg AT, Zellner JL, and Crumbley AJ. A matrix metalloproteinase induction/activation system exists in the human left ventricular myocardium and is upregulated in heart failure. *Circulation* 102: 1944-1949, 2000.

50. Suzuki G, Iyer V, Lee T, and Canty JJ. Intracoronary injection of autologous mesenchymal stem cells (MSCs) increases the myocardial localization of CD133+ hematopoietic stem cells (HSCs) in swine with hibernating myocardium. *Circulation* 116 (Suppl II): II-133, 2007.
51. Suzuki G, Lee TC, Fallavollita JA, and Canty JM, Jr. Adenoviral gene transfer of FGF-5 to hibernating myocardium improves function and stimulates myocytes to hypertrophy and reenter the cell cycle. *Circ Res* 96: 767-775, 2005.
52. Takahashi M, Li TS, Suzuki R, Kobayashi T, Ito H, Ikeda Y, Matsuzaki M, and Hamano K. Cytokines produced by bone marrow cells can contribute to functional improvement of the infarcted heart by protecting cardiomyocytes from ischemic injury. *Am J Physiol Heart Circ Physiol* 291: H886-893, 2006.
53. Tang YL, Zhao Q, Qin X, Shen L, Cheng L, Ge J, and Phillips MI. Paracrine action enhances the effects of autologous mesenchymal stem cell transplantation on vascular regeneration in rat model of myocardial infarction. *Ann Thorac Surg* 80: 229-236, 2005.
54. Tateno K, Minamino T, Toko H, Akazawa H, Shimizu N, Takeda S, Kunieda T, Miyauchi H, Oyama T, Matsuura K, Nishi J, Kobayashi Y, Nagai T, Kuwabara Y, Iwakura Y, Nomura F, Saito Y, and Komuro I. Critical roles of muscle-secreted angiogenic factors in therapeutic neovascularization. *Circ Res* 98: 1194-1202, 2006.
55. Terada N, Hamazaki T, Oka M, Hoki M, Mastalerz DM, Nakano Y, Meyer EM, Morel L, Petersen BE, and Scott EW. Bone marrow cells adopt the phenotype of other cells by spontaneous cell fusion. *Nature* 416: 542-545, 2002.
56. Tegel F, Hu Z, Weiss K, Isaac J, Lange C, and Westenfelder C. Administered mesenchymal stem cells protect against ischemic acute renal failure through differentiation-independent mechanisms. *Am J Physiol Renal Physiol* 289: F31-42, 2005.
57. Tyndall A, Walker UA, Cope A, Dazzi F, De Bari C, Fibbe W, Guiducci S, Jones S, Jorgensen C, Le Blanc K, Luyten F, McGonagle D, Martin I, Bocelli-Tyndall C, Pennesi G, Pistoia V, Pitzalis C, Uccelli A, Wulffraat N, and Feldmann M. Immunomodulatory properties of mesenchymal stem cells: a review based on an interdisciplinary meeting held at the Kennedy Institute of Rheumatology Division, London, UK, 31 October 2005. *Arthritis Res Ther* 9: 301, 2007.
58. Uemura R, Xu M, Ahmad N, and Ashraf M. Bone marrow stem cells prevent left ventricular remodeling of ischemic heart through paracrine signaling. *Circ Res* 98: 1414-1421, 2006.
59. Vacanti V, Kong E, Suzuki G, Sato K, Canty JM, Jr., and Lee T. Phenotypic changes of adult porcine mesenchymal stem cells induced by prolonged passaging in culture. *J Cell Physiol* 205: 194-201, 2005.
60. Vulliet PR, Greeley M, Halloran SM, MacDonald KA, and Kittleson MD. Intra-coronary arterial injection of mesenchymal stromal cells and microinfarction in dogs. *Lancet* 363: 783-784, 2004.
61. Widimsky P, and Penicka M. Complications after intracoronary stem cell transplantation in idiopathic dilated cardiomyopathy. *Int J Cardiol* 111: 178-179, 2006.

62. Yoon YS, Park JS, Tkebuchava T, Luedeman C, and Losordo DW. Unexpected severe calcification after transplantation of bone marrow cells in acute myocardial infarction. *Circulation* 109: 3154-3157, 2004.
63. Zou Y, Takano H, Mizukami M, Akazawa H, Qin Y, Toko H, Sakamoto M, Minamino T, Nagai T, and Komuro I. Leukemia inhibitory factor enhances survival of cardiomyocytes and induces regeneration of myocardium after myocardial infarction. *Circulation* 108: 748-753, 2003.

Figure Legends

Figure 1. Cardiac functional improvement by intramuscular injection of MSCs and MSC-conditioned medium. A & B: %FS and LVDd at pre-injection and one month post injection (n = 5 per group) were obtained by blind-folded echocardiography. MSCs at the indicated cell dosages were injected into the hamstring muscles of 4-month old TO2 hamsters. Control TO2 hamsters received HBSS injections. Normal F1B hamsters were not injected, and were shown as a reference for panels A-D. C & D: %FS and LVDd before and one month after the first intramuscular injection of MSC-conditioned medium vs. control medium (n = 4 per group). The MSC-conditioned medium used here were from the same batch. Note that the 0.25-million MSC group exhibited a higher mean %FS at pretreatment than the 1-million MSC group. MSC-mediated improvements in %FS between the two cell dosage groups were statistically similar after normalization to the pretreatment level. * P<0.05 vs control; ** P<0.01 vs control; *** P<0.001 vs control; #P<0.05 vs pre-treatment; ##P<0.01 vs pre-treatment; ###P<0.001 vs pre-treatment.

Figure 2. Increased capillary and myocyte nuclear densities after MSC administration. A: representative images of capillary and myocyte staining using FITC-labeled GSL-IB4 lectin (green) and TnI antibody (red), respectively. DAPI (blue) was used for nuclear staining. B & C: computer analysis of capillary and myocyte nuclear densities expressed as numbers per mm². D: Computer analysis of myocyte cross-section diameters. At least fifteen 200x fields and greater than 350 myocytes were evaluated in each hamster. E: a frequency histogram of diameters showing a greater number of smaller myocytes in the

MSC-treated group (n = 4 per group). * P<0.05 vs control; ** P<0.01 vs control; *** P<0.001 vs control.

Figure 3. MSC administration augments cell cycle activities in the myocardium. A: a representative image of Ki67⁺ cells (pink nuclei). Myocytes were stained by a TnT antibody (green). Nuclei were stained by DAPI (blue). B & C: % Ki67⁺ myocytes and % total Ki67⁺ nuclei (n=4 per group). D: a representative image of phosphohistone H3 (p-HH3)-positive cells (pink nuclei). E & F: % p-HH3⁺ myocytes and % total p-HH3⁺ nuclei (n=4 per group). * P<0.05 vs control.

Figure 4. MSC administration reduces myocardial apoptosis and tissue damage. A & B: % myocyte and non-myocyte apoptosis. At least twenty-five 200x fields and greater than 8,000 cells were evaluated in each hamster. C: decreased circulating levels of cTnI after MSC administration (n = 3 per group). * P<0.05 vs control; ** P<0.01 vs control.

Figure 5. Attenuation of myocardial fibrosis by MSCs. A: H&E-stained (top) and Trichrome-stained (bottom) heart sections. B: quantification of fibrotic areas (n = 5 per group). C: qRT-PCR analysis of expression of genes involved in extracellular tissue remodeling. Results were representatives of two independent experiments. * P<0.05 vs control; ** P<0.01 vs control; *** P<0.001 vs control; †P<0.001 vs F1B.

Figure 6. Increased circulating and myocardial trophic factors. A: circulating (plasma) levels of HGF, LIF and M-CSF one month after MSC administration (n = 3 per group).

B: heart tissues were collected one month after MSC administration, and homogenized. Clarified lysates were assayed by HGF, IGF-2, and VEGF ELISA kits (n = 4 per group).

* P<0.05 vs HBSS control.

Figure 7. Mobilization of bone marrow progenitor cells. Circulating c-kit⁺, CD133⁺, and CD31⁺ cells were quantified by flow cytometry three days after MSC injections. Cell numbers per million peripheral blood mononuclear cells were presented (n = 3 per group). * P<0.05 vs control.

Figure 8. Increased myocardial c-kit⁺ progenitor cells. A: representative images of interstitial c-kit⁺ cell (red). Myocytes were stained by a TnT antibody (green). Nuclei were stained by DAPI (blue). B: quantification of c-kit⁺ cells. C: qRT-PCR confirmed the quantification data in panel B. Note that expression of CD45 (leukocyte common antigen) was not affected by MSC administration. **P<0.01 vs HBSS control.

Table 1. Primer sequences for qRT-PCR

Gene	Forward Primer	Reverse Primer
Beta-2-Microglobulin (β 2M)	TCTCTTGGCTCACAGGGAGT	ATGTCTCGTCCCAGGTGAC
c-kit	GCCACGTCTCAGCCATCTG	GTCGCCAGCTTCAACTATTA
HGF	AGAGGTCCCATGGATCACAC	AGCCCTTGTCGGGATATCTT
IGF-2	CAAGTCCGAGAGGGATGTGT	GGACTGTCTCCAGGTGTCGT
VEGF	TCACCAAAGCCAGCACATAG	AAATGCTTTCTCCGCTCTGA
Col1 α 1	GAGCGGAGAGTACTGGATCG	GTTTCGGGCTGATGTACCAGT
Col1 α 2	CGAGACCCTTCTCACTCCTG	GCATCCTTGTTAGGGTCAA
Col3 α 1	GGGATCCAATGAGGGAGAAT	GGCCTTGCGTGTTTGATATT
MMP-13	TTTATTGTTGCTGCCCATGA	AACTGGATTCCTTGCACGT
MMP-2	TGGTTTCCCTAAGCTCATCG	TTGGTTCTCCAGCTTCAGGT
MMP-9	GTCTTCCCCTTCGTCTTCCT	CACTTCTTGTGAGCGTCGAA
CD45	GGCGTACAGGCACCTACATT	ATGTAAGGGCCTCCACTTG
TIMP 1	CATGAAAGCCTCTGTGGAT	CTCAGAGTACGCCAGGGAAC
TIMP 2	GACTGGGTCACGGAGAAGAG	GGGCCTCGATGTCAAGAAA
TIMP 3	GCTGTGCAACTTTGTGGAG	GGTCACAAAGCAAGGCAAG

Fig 1

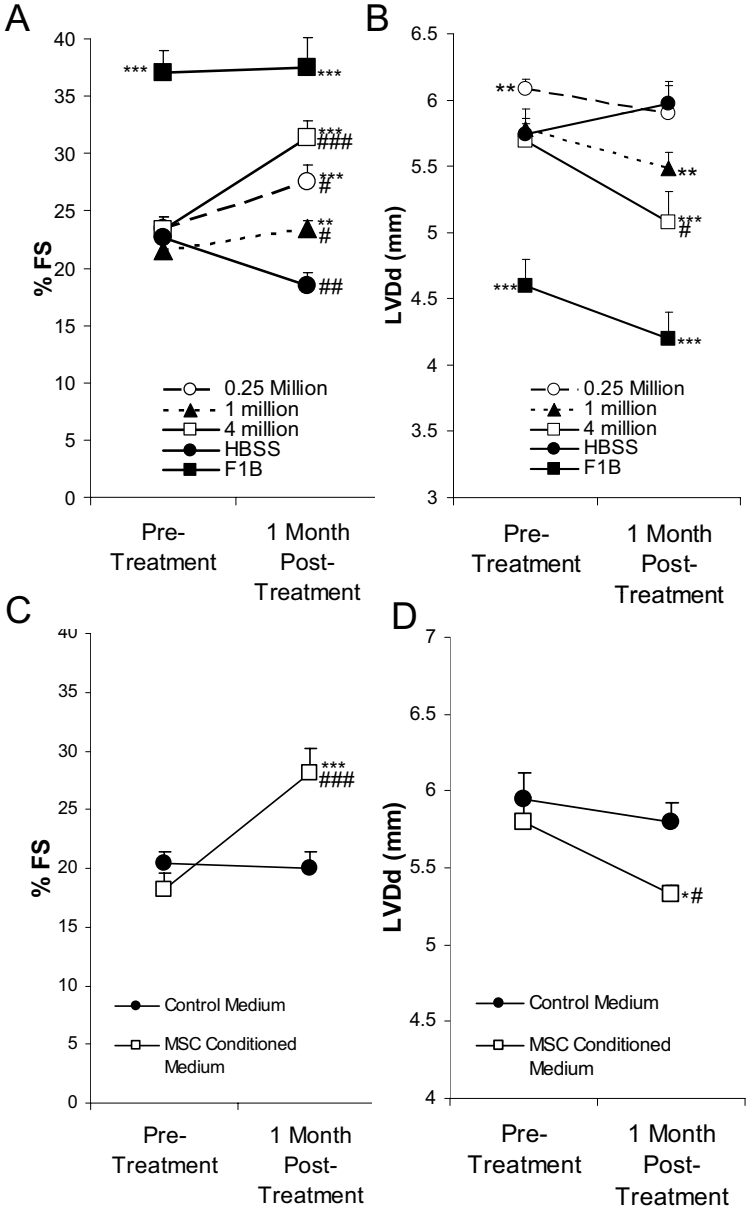


Fig 2

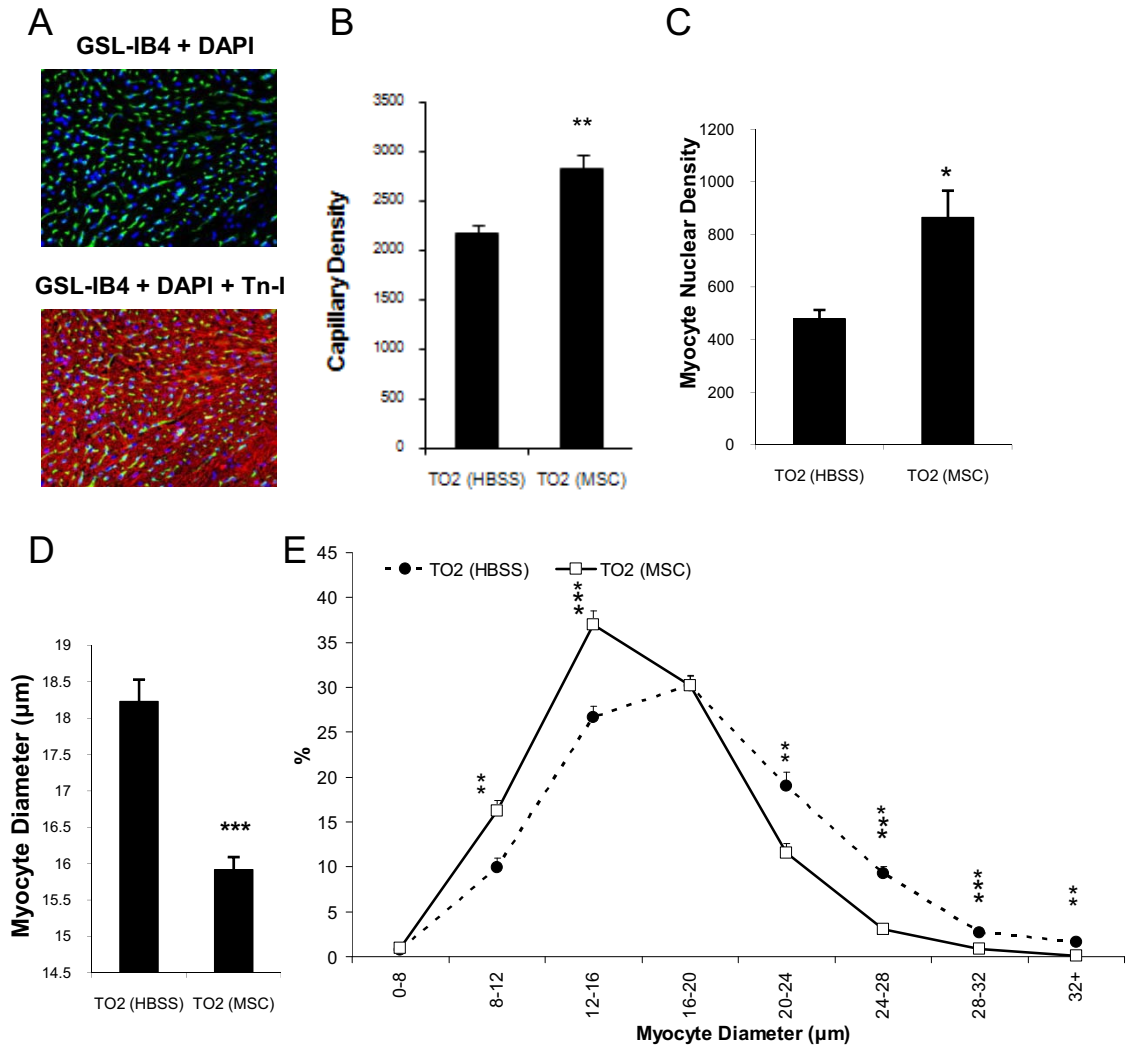


Fig 3

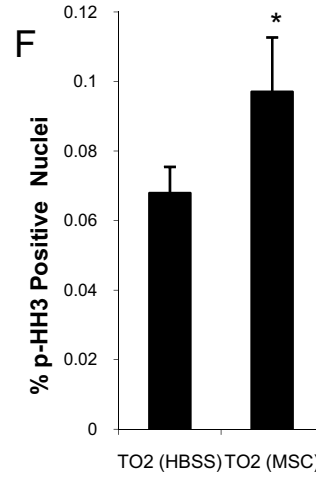
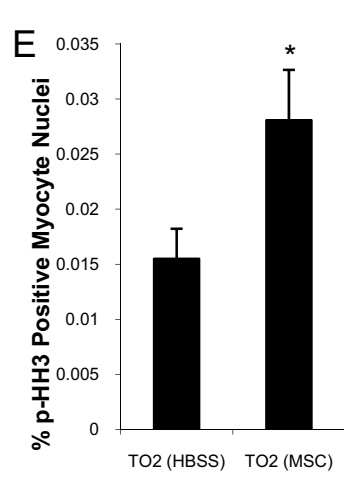
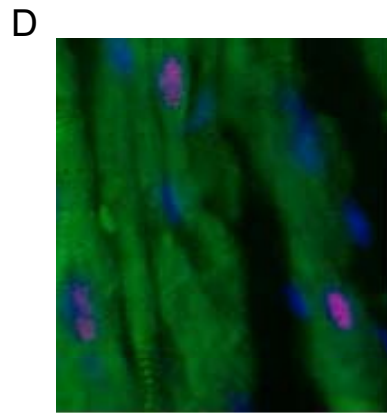
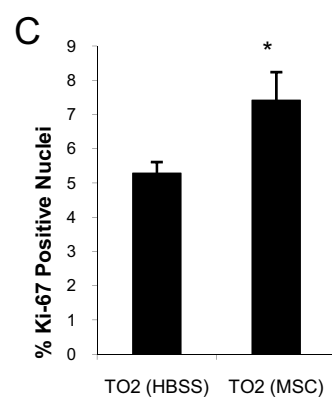
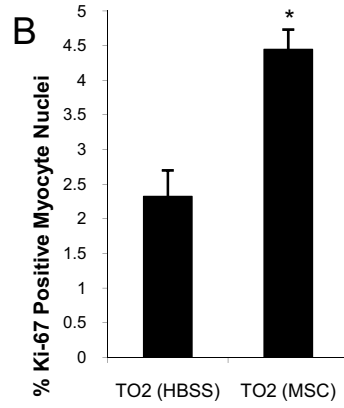
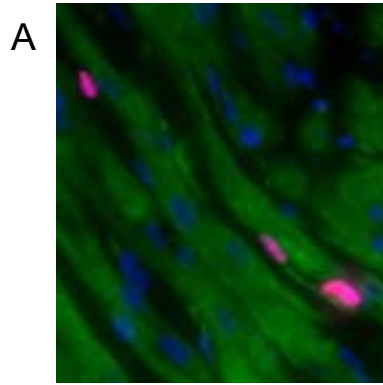


Fig 4

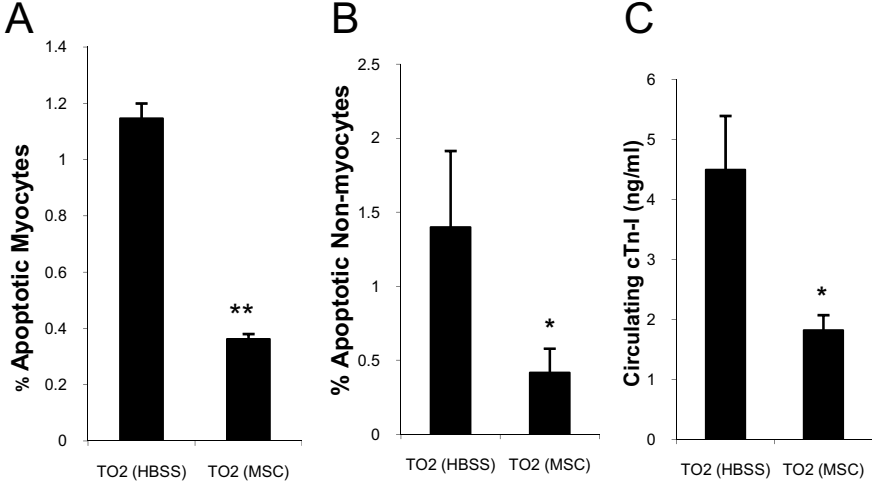


Fig 5

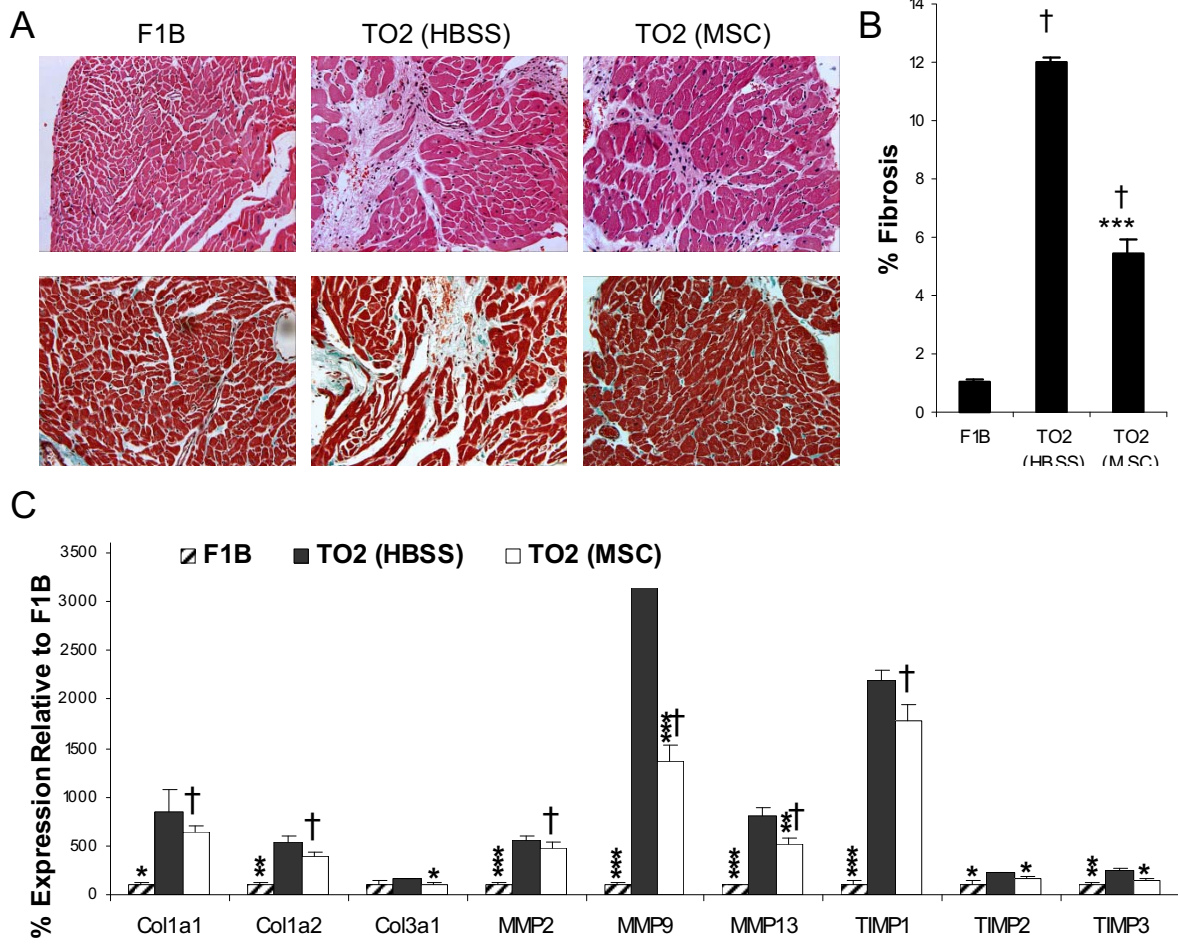


Fig 6

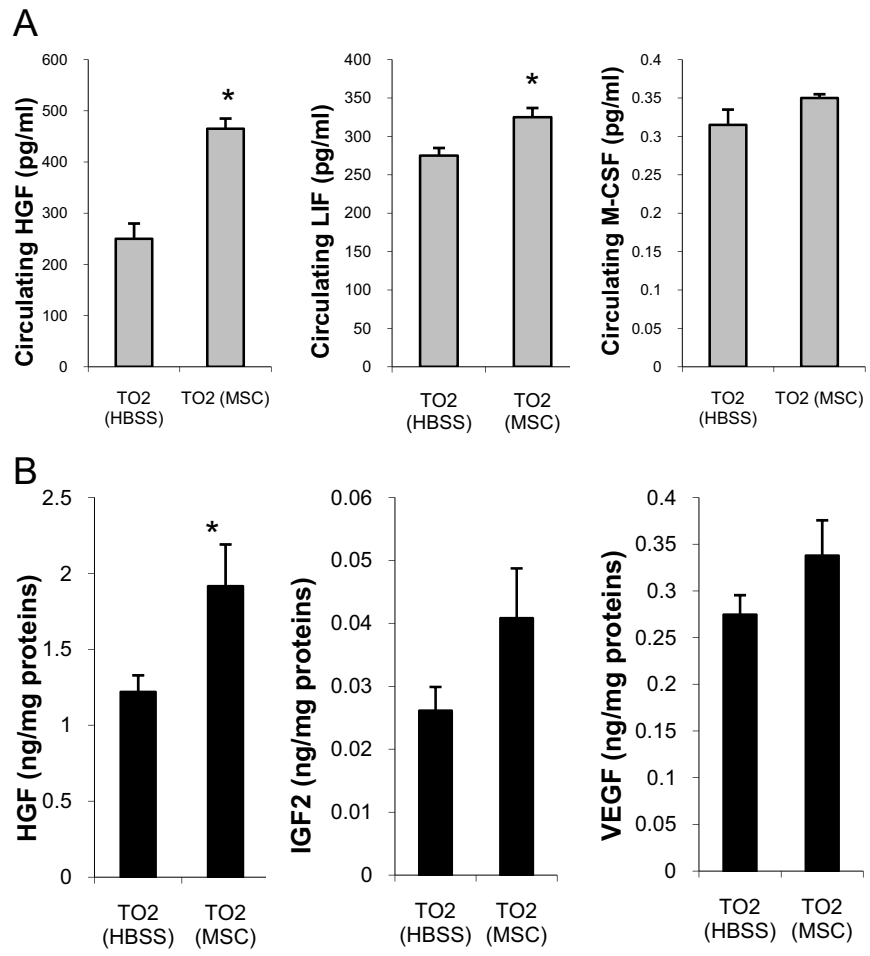


Fig 7

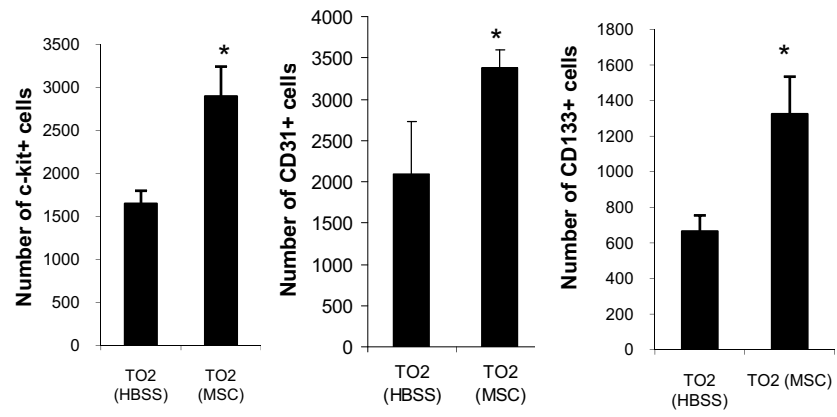


Fig 8

